PCCP

Accepted Manuscript

ROYAL SOCIETY OF CHEMISTRY

www.rsc.org/pccp

PCCP

ARTICLE

Imidazole tailored deep eutectic solvents for CO_2 capture enhanced by hydrogen bond

Received 00th XXX 2015,
Accepted 00th XX 2015

DOI: 10.1039/x0xx00000x

www.rsc.org/

Lingdi Cao,[a,b,c] Junhua Huang,[c, d] Xiangping Zhang,[a] Suojiang Zhang,*[a] Jubao Gao,[a] and Shaojuan Zeng[a, b]

Deep eutectic solvents (DESs) are emerging alternatives as promising candidates for CO_2 capture in recent years. In this work, several novel DESs were firstly prepared to enhance CO_2absorption. Structural and physical properties of DESs were investigated, as well as their absorption performance of CO_2. A distinct depression in melting point up to 80 K of DESs was observed compared with that of BMIMCl. The observed red shifts of C_2H group in imidazolium ring and its chemical shifts to a downfield in NMR spectra are indicative of hydrogen bond interaction between BMIMCl and MEA. In particular, CO_2 uptake in MEA:ILs(4:1) at room temperature and atmospheric pressure is up to 21.4 wt%, which is higher than that of 30 wt% MEA (13%). A hydrogen bond related mechanism was proposed in whichILs act as medium improving CO_2 uptake through hydrogen bond. Finally, the firstly reported overall heat of CO_2 absorption is slightly higher with that of 30 wt% MEA, implying that the hydrogen bond of DESs contributes to the over heat of CO_2 absorption. This study reveals that the heat of CO_2 absorption can be tailored with proper molar ratio of MEA and ILs.

1 Introduction

Issues arising from fossil fuel derived CO_2 accumulation are causing intense environmental concern. Urgent reduction of the emissions of CO_2 is necessary for the mitigation of global climate change.[1] From the existing capture strategies, the proven and mature technology is chemical absorption using aqueous amine solutions.[2, 3] Aqueous solution of monoethanolamine (MEA) was widely used for CO_2 absorption with many advantages such as lower costs, high efficiency, and satisfactory absorption capacity.[4, 5] However, the major problem of MEA technology is that this method has significant energy consumption during the solvent regeneration process.[2, 6] Other drawbacks include solvent degradation and evaporation, corrosion, foaming, and fouling.[7, 8] These drawbacks limit the amine concentration and lead to high capture cost. Therefore, it is highly desired to develop alternative solvent to improve capture efficiency and to reduce capture cost.

In this context, ionic liquids (ILs) have garnered considerable interests in developing new generation technologies for CO_2 capture.[9-11] ILs are deemed as alternatives for CO_2 capture because they are "designable solvents" exhibiting truly unique physical properties and finely tuned structures.[12-15] Not surprisingly ILs have demonstrated beneficial in industrial processes like BASIL™ process[16], showing good potential for handling at industry scale.[17, 18] To date, many kinds of ILs have been designed for CO_2 capture.[19-26] Their remarkable non-volatility, thermal stability and low heat capacity make ILs energetically more efficient in desorption processes where CO_2 rich solvents are heated to release CO_2. However, the CO_2 uptake of the common ILs is very low on a weight basis. As for the functionalized ILs, although their CO_2 uptake can be greatly improved by incorporating suitable functionalities, the synthesis of ILs needs several steps and the subsequent purification are troublesome. Also, there remain other issues employing ILs for carbon capture, including their inherent high costs, high viscosity[27] and slow mass transfer of CO_2.[19, 25]

Recently, deep eutectic solvents (DESs) have been a focal point as an emerging solvents and are versatile alternatives to ILs.[11, 28-36] DESs are deemed as an alternative approach to ILs because DESs share most of their good qualities while overcome the limitations of ILs cousins.[37] DESs are typically less expensive, nontoxic, biodegradable and more synthetically accessible.[38] Preparation of DESs could be simply mixing constituent components under mild heating, requiring no further purification steps. The resultant DESs normally contains cations, anions and neutral molecules. Consequently, DESs have the characteristics of both ionic and molecular solvents, generating interesting properties that are not exhibited by either ILs or molecular analogues alone. DESs are

[a] Beijing Key Laboratory of Ionic Liquids Clean Process, State Key Laboratory of Multiphase Complex Systems, Key Laboratory of Green Process and Engineering, Institute of Process Engineering, Chinese Academy of Sciences, Beijing 100190, China.
[b] College of Chemistry and Chemical Engineering, University of Chinese Academy of Sciences, Beijing 100049, China.
[c] CSIRO Energy Technology, Clayton South, VIC 3169, Australia.
[d] School of Chemistry, Monash University, Clayton, VIC 3800, Australia

† Footnotes relating to the title and/or authors should appear here.
Electronic Supplementary Information (ESI) available: Thermal properties, characterization of sample and the experimental setup. See DOI: 10.1039/x0xx00

mixtures of two or more components characterized by a lower freezing point than those of individual constituents, attributed to the formation of hydrogen bonds between the constituents.[39] Usually, DESs shows lower viscosity than many kinds of ILs, especially functionalized ones. After Abbott *et al*[28, 29] first developed a variety of DESs that have potential application for metal extraction, DESs have been increasingly studied for CO_2 capture,[40-43] due to some favourable characteristics such as negligible vapor pressure and good CO_2 affinity. Li *et al*[32] studied the CO_2 solubility in choline chloride/urea DESs at different temperature and pressures up to 13 MPa. The solubility of CO_2 in the DESs with the molar ratio of 1:2 for choline chloride/urea is 0.309 at 313 K and 12.5 MPa. Afterwards, Su *at al*[44] investigated the solubility of CO_2 in ternary DESs (ChCl/urea/H_2O). Very recently, Li's group studied the solubility of CO_2,[32, 45, 46]diffusivity[47] and molar heat capacities[48] of choline chloride based DESs. Their results shows that the solubility of CO_2 are 0.2694 mol·kg^{-1} (~1.19wt%) in 1:2 choline chloride–urea DESs at 313.15 K and 350 kPa and 0.1103 mol·kg^{-1} (~0.49wt%) in 1:2 choline chloride–glycerol DESs at 313.15 K and 191 kPa, respectively. These results show that the CO_2 solubility in DESs increases as the content of H_2O decreases. It is found that the solubility of CO_2 is comparable with those of common ILs and still lower than that of aqueous solution of MEA. Imidazolium based ILs have been reported to have good CO_2 solubility and selectivity for CO_2 capture.[49-51] Bara *et al* demonstrated that imidazolium based systems show attractive potentials for chemical engineering processes.[52, 53] Interestingly, chloride ion has been reported to stabilize CO_2 adducts of ILs, resulting in higher CO_2 uptake.[54] It has been established that the C2–H···X interaction is considerably different from conventional hydrogen bonds[55, 56] which has a significant impact on the physical properties of ILs.[57, 58] However, there is little information available on the hydrogen bond interaction influencing the CO_2 absorption using DESs.

Information on the reaction heat of CO_2 in solvents is of great significance for gas removal because it is closely related to the requirements of regeneration step. Therefore, it is desirable that the enthalpy of CO_2 absorption should be low and that the data should be accurate. It is well known that the enthalpy can be estimated from vapor liquid equilibrium data by virtue of the Gibbs-Helmholtz equation.[40, 59] However, it is reported that the uncertainty of the reaction heat estimated using Gibbs-Helmholtz equation can be around 20-30%.[60] Therefore, direct calorimetric measurements of enthalpy reflect the heat effects coming from the physical dissolution of CO_2 and the chemical reaction between CO_2 and solvent.

As highlighted above, the CO_2 uptake in existing DESs are still low. Still, no direct experimentally measured heat of CO_2 absorption in DESs has been reported to date. To improve the absorption capacity of CO_2, several BMIMCl based DESs were synthesized. The hydrogen bond interaction existed in DESs was analyzed. In addition, the absorption performance and mechanism of CO_2 in these DESs were studied. Finally, the thermal and physical properties of these imidazolium based eutectics, such as melting point (T_{fus}), glass transition temperatures (T_g), decomposition temperature (T_d), heat capacities (C_P), density and viscosity were measured.

Experimental

Materials

1-butyl-3-methylimidazolium chloride (BMIMCl) (Merck > 99%) and monoethanolamine (MEA) (Merck ≥ 99%) were directly used without further purification. Ultrapure CO_2 was supplied by BOC Limited, Australia.

Preparation and characterization

The procedures to prepare eutectic mixtures were similar to those reported in the literature.[28, 29, 61] Typically, the eutectic mixture was prepared by mixing BMIMCl and MEA in a 25 mL round-bottom-flask under Argon atmosphere. Then the mixture was heated and stirred at 358 K for ~2 hours. A homogeneous, colorless and transparent liquid was produced. For convenience, abbreviations of MEA:ILs(1:1), MEA:ILs(2:1) and MEA:ILs(4:1) stand for the DESs with the MEA/ILs molar ratios of 1:1, 2:1 and 4:1. It should be noted that, due to the high hygroscopicity of HBD and organic salt, precautions must be taken to avoid the exposure to air moisture. The eutectic solvent was transferred into an NMR tube using tetradeuteromethanol (CD_3OD) as reference solvent and then characterized by ^1H and ^{13}C NMR (BrukerAV400X) at room temperature and ambient pressure. Infrared spectra in the range of 4000 – 500 cm^{-1} of the samples were obtained on a Perkin-Elmer Spectrum 400 ATR-IR instrument (Waltham, MA) with an ATR force gauge (Shelton, CT). Raman spectra were collected using a Perkin-Elmer 400F Spectrometer.

Density and viscosity

Densities (ρ) of the mixtures were measured from 293 K to 333 K using an Anton Paar DMA 4500. The reproducibility of density data was ± 10^{-6}g·cm^{-3} and the accuracy of density measurements was ± 5×10^{-6}g·cm^{-3}. Viscosity (η) of the mixtures were determined using an Anton PaarAMVn viscometer with a repeatability < 0.1%. The viscosity of each sample was measured four times and the average value was reported.

Thermal properties

Melting point (T_m) and glass transition temperatures (T_g) were determined using a Mettler Toledo Differential Scanning Calorimetry (DSC) 2010 instrument. The DSC operating temperature ranges from 133 to 423 K and the purge gas was nitrogen with a flow rate at 40 mL·min^{-1}. The detailed procedures were reported elsewhere.[48, 62] Decomposition temperature (T_d) was investigated using a TA thermogravimetric analyzer (TGA) 2050 under a nitrogen atmosphere. In a typical run, the sample was loaded on to an aluminium pan under a nitrogen atmosphere and was then heated at a rate of 10 K·min^{-1} from 298 to 473 K. Reproducibility was verified by three runs. The onset temperature at the intersection of the baseline weight and the tangent of the weight loss was taken as T_d. Heat capacity was measured at 1 K·min^{-1} from room temperature to 358 K, using

sapphire with known heat capacity as a reference material.[63] The overall error was estimated to be within ± 4 %.[64]

CO_2 absorption

CO_2 absorption performance in these eutectic solvents was investigated using a weighing method similar to the previous publications.[23, 25] The absorption experiment was conducted with stirring at room temperature and atmospheric pressure. In a typical run, CO_2 was continuously introduced into a one-neck round bottom flask (*ca*. 25 mL) loaded with 1-2 g solvent. The mass change was recorded at designed intervals using an analytical balance with an accuracy of 0.1 mg until the absorption equilibrium was reached. CO_2 absorption experiment for each sample was repeated three times. In this work, CO_2 absorption in neat MEA and the commonly used 30% w/w aqueous solution were carried out to establish baselines for comparison.

Heat of CO_2 absorption

The overall enthalpy of CO_2 absorption in DESs at 313 K are determined using an isothermal calorimeter Setaram BT 2.15, which is widely used for the heat measurement.[59] The experimental setup of the reaction calorimeter is shown in Fig. S12. The detailed experimental procedures are can be found in our previous work.

Results and discussion

Characterization of DESs

The IR spectra of pure MEA, BMIMCl and DESs are presented in Fig. 1. In the infrared spectrum of MEA, O-H stretching vibration appears at 3350 cm^{-1} and N-H stretching vibration appears at 3285 and 3163 cm^{-1}, as shown in Fig. 1. The C-H stretching vibrations of the ethyl occur at 2921 and 2852 cm^{-1}. N-H bending, C-H scissors, C-N stretching and C-O stretching vibrations of MEA are ascribed at 1597, 1457, 1076, and 1031 cm^{-1}, respectively. In case of BMIMCl, the cation of imidazolium is well studied.[65-67] In the region of 3000 to 3160 cm^{-1}, several bands are assigned to the aromatic C-H stretching vibrations on the imidazolium ring. Two peaks at 3152 cm^{-1} and 3113 cm^{-1} are assigned to the symmetric and antisymmetric stretching modes of $C_4(_{or5})$-H. The peak at 3091 cm^{-1} is ascribed to the vibration of C_2-H. Two peaks at 2999 and 3016 cm^{-1} are attributed to the symmetric and antisymmetric stretch mode of the methyl group attached to the imidazolium ring. In the region from 2800 to 3000 cm^{-1}, the peaks at 2967, 2950, 2935, 2872 and 2850 cm^{-1} are assigned to the C-H stretching modes of the butyl chain. The absorption peak at 1173 cm^{-1} is a characteristic peak of the $BMIM^+$ cation.[51] The bands between 700 and 1000 cm^{-1} are nominated as the bending modes of imidazolium ring.

Generally, the infrared spectra of DESs exhibit the characteristic bands of both MEA and ILs. The broad peak at ~3270 cm^{-1} can mainly be attributed to the broadening of O-H and N-H stretching of MEA, indicating the formation of hydrogen bond between MEA and ILs; whilst the two narrow and weak peaks at ~3140 and 3065 cm^{-1} are nominated as the aromatic C-H stretching vibration of imidazolium ring accompanied by the aliphatic C-H stretching below 3000 cm^{-1}.[1, 66, 68, 69] Quantum chemical calculations have demonstrated that the formation of hydrogen bond of the C-H.[70, 71]The red-shifted bands of the $C_4(_5)$-H from 3152 to ~3140 cm^{-1} and C_2-H from 3091 to 3065 cm^{-1} upon mixing with MEA, possibly suggesting forming hydrogen bond between the hydrogens on the ring and MEA.[72, 73] C_2-H shows a bigger red shift up to 26 cm^{-1} than $C_4(_5)$-H, implying that C_2-H group is more strongly involved in hydrogen bond. Recent work on imidazolium based ILs suggests that C_4-H and C_5-H also participate in hydrogen bond in addition to C_2-H;[57, 68, 72] Nevertheless C_2-H hydrogen bond affects stabilization more than those of C_4-H and C_5-H. That is because C_2 on imidazolium ring is positive because of electron deficient C=N π bond formation, while C_4 and C_5 are basically neutral because of C=C π bond formation.[74] Previous studies have demonstrated that the peaks in the region of 3100-3200 cm^{-1} are the interactions are produced by Fermi resonances with the combination and overtone peaks of the imidazolium ring vibrations and C-H stretching modes.[75] It is believed that increasing strength of ahydrogen bond leads to a shorter bond distance and larger force constants.[73] As these bands show, the stronger hydrogen bond results in lower wavenumber of the vibrational peaks.

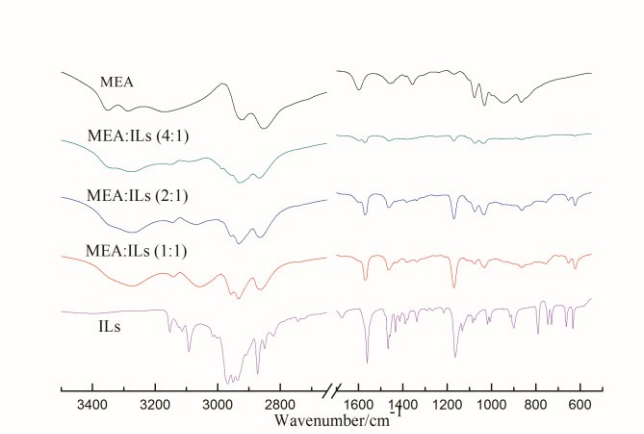

Fig. 1 IR spectra of MEA, BMIMCl and DESs.

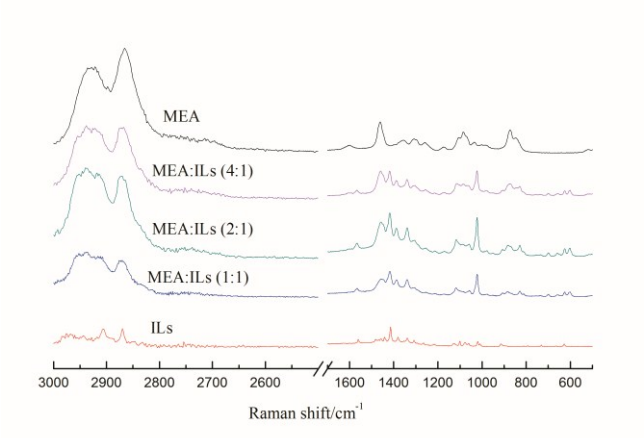

Fig. 2 Raman spectra of MEA, BMIMCl and DESs.

Also, it is easy to find the red-shifts of alkyl groups in the region of 2800 and 3000 cm^{-1} which results from the formation of hydrogen bond between ILs and amine. Finally, an important shoulder peak at ~1560 cm^{-1} attributed to the N-H bending of MEA appears in the spectra of DESs. The peak is less obvious for MEA:BMIMCl (1:1). Therefore, it is concluded that the hydrogen bond most likely forms through NH_2 group and C_2-H group.

The Raman spectra for MEA, BMIMCl and DESs are shown in Fig. 2. The structural vibrations of BMIMCl and MEA in this study are in agreement with those in literatures.[76, 77] As for the Raman spectrum of pure BMIMCl, the signals in the region of 2760-3000 cm^{-1} are ascribed to the C-H vibrations of the alkyl chains. The band at 1560 cm^{-1} is ascribed to the ring in-plane symmetric/asymmetric stretch. The spectrum region of 1216~1338 cm^{-1} are attributed to the stretching vibrations of butyl group, whilst those in the region of 1441~1481 cm^{-1} are attributed to the symmetric bending of butyl group and ring in-plane asymmetric stretching vibrations.[78] With respect to the peak at ~1060 cm^{-1}, it is assigned to the asymmetric vibration of ring C-N stretching. According to Holomb et al,[79] the peaks in the region of 800-1000 cm^{-1} are characteristic bands for $BMIM^+$ conformers. Previous work has demonstrated that BMIMCl has two crystal forms, namely, monoclinic and orthorhombic crystal,[76] which was confirmed by XRD that the main structural difference between the two crystals stems from the rotational isomerism around C_7-C_8 bond of the butyl group.[80] In other words, the monoclinic crystal corresponds to the *trans* conformation and orthorhombic crystal corresponds to *gauche*. The Raman spectrum of BMIMCl in this study shows three characteristic peaks: 627 cm^{-1} for $CH_3(N)CN$ stretching, 731 cm^{-1} for $CH_3(N)CN$ bending and 792 cm^{-1} for NC(H)N out-plane bending vibrations, which suggests that a monoclinic crystal, a more thermodynamically stable form, was obtained in our study. For the spectrum of MEA, the C-H stretching and N-H bending vibration can be assigned at 2800~2950 cm^{-1} and 1600 cm^{-1}, respectively. The sharp band at 1460 cm^{-1} is the asymmetric vibration of CH_2 group adjacent to the NH_2 group. The bands in 1330-1380 cm^{-1} are the stretching vibrations of OCH and NCH of MEA. The bands at 872 cm^{-1} can be nominated as the C-C vibration. The bands at 516 and 481 cm^{-1} are respectively attributed to the antisymmetric skeletal deformation vibration of the *gauche* form and symmetric skeletal deformation vibration of the *trans* form.[81] Compared with pure BMIMCl and MEA, the spectrum of DESs shows obvious difference. Firstly, the obvious band at 1600 cm^{-1}, corresponding to NH_2 group of MEA, disappears after mixed with ILs, accompanying with a slight blue shift of imidazole ring in ILs from 1560 to 1565 cm^{-1} in DESs. Importantly, the peaks at 1417, 1386, 1339 and 1022 cm^{-1} originating from the characteristic band of C-N ring stretching in DESs become intensified, which is indicative of the formation of hydrogen bond interaction through the H on the C_2 and NH_2 group from MEA.[82]

^{1}H NMR and ^{13}C NMR spectra, shown in Fig. 3 and Fig. 4, provide further evidence of the interaction between BMIMCl and MEA. The ^{1}H NMR spectra of pure MEA and BMIMCl are in good agreement with the previous studies.[83, 84] As Fig. 3 shows, pure MEA has two triple peaks at 3.54 and 2.69 ppm, which corresponding to the OCH_2 and NCH_2 groups respectively. For pure BMIMCl, the chemical shifts at 9.03, 7.67 and 7.59 ppm are assigned to C_2H, C_4H and C_5H groups, respectively. Seddon and the co-workers, using NMR, revealed that three hydrogen atoms on imidazole ring can form hydrogen bond and a quasi-molecular state, showing a conventional aromatic stacking phenomenon.[72] In this work, the C_2 hydrogen in DESs shifts to downfield as the composition changed with the addition of MEA, e.g. from 9.03 ppm in BMIMCl to 9.15 ppm in MEA:ILs(1:1) and to 9.14 ppm in MEA:ILs(2:1). This is the evidence of forming hydrogen-bonded complex between MEA and ILs.[68, 85] The C_2 hydrogen is acidic and can introduce a strong localized and highly directional hydrogen bond. The downfield shifts in ^{1}H NMR indicate lower electron density and stronger interionic interaction through forming hydrogen bond. This leads to asymmetric electron redistribution on imidazolium ring. Previous work found that C_4 and C_5 hydrogens on imidazolium ring are capable of forming shorter hydrogen bond than C_2 hydrogen.[57, 68, 72]

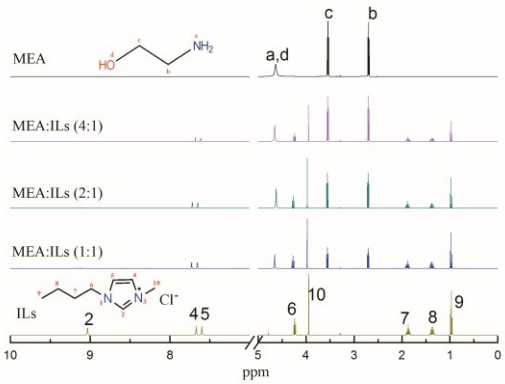

Fig. 3 ^{1}H NMR spectra of MEA, BMIMCl and DESs.

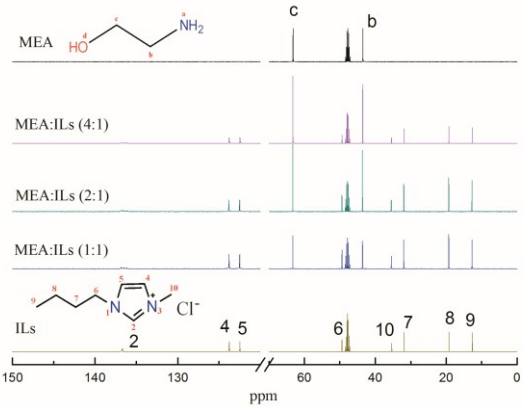

Fig. 4 ^{13}C NMR spectra of MEA, BMIMCl and DESs.

Fig. 3 shows that the signals at C_4 and C_5 hydrogen in the DESs also shift to downfield, *e.g.*, from 7.67 to 7.74 ppm and from 7.59 to 7.62 ppm for MEA:ILs(1:1), respectively. The smaller downfield shifts of C_4 and C_5 hydrogen than C_2 are due to the influence of the two nitrogen atoms of the ring on C_2, as nitrogen atoms on imidazolium ring can withdraw electron due to their higher electron negativity compared with carbon atoms. This again suggests that hydrogen bonds form between $BMIM^+$ and amine.

The representative ^{13}C NMR spectra were presented in Fig. 4. As shown in Fig. 4, the ^{13}C NMR spectra of fresh MEA shows two peaks at 43.5 ppm ($-CH_2NH_2$) and 63.0 ppm ($-CH_2OH$), respectively.[83, 86] In case of pure BMIMCl, C_2, C_4 and C_5 can be found at 136.6, 123.7 and 122.4 ppm.[84, 87] Other signals can be ascribed to the alkyl chains. For the ^{13}C NMR spectra of DESs, all the intuitively expected signals correspond to those of pure MEA and BMIMCl. No new signals and distinct shifts can be observed in ^{13}C NMR spectra of DESs.

Density and viscosity of DESs

Densities and viscosity of the DESs were measured at atmospheric pressure as a function of temperature ranging from 278.15 K to 343.15 K. The experimental densities and viscosities *vs* temperature are plotted in Fig. 5 and 6. In order to confirm the reliability of the data, viscosity and density of MEA were determined and compared with those of literature.[88, 89] As Fig. 5 and Fig. 6 show, the experimental and the literatures data show good consistency for density and viscosity of MEA. As expected, density and viscosity of the DESs decrease with increasing temperature. The densities of all DESs investigated decrease linearly with increasing temperature, as depicted in Fig. 5. All DESs and pure individuals exhibit slightly higher densities than those of pure water at given temperatures.

The viscosity and temperature profiles indicate an Arrhenius behavior, as Fig. 6 shows. The viscosity of the DESs decrease markedly with increasing temperature: the viscosity of MEA:ILs(1:1) is 130.223 mPa·s at 298 K, being one order of magnitude higher than 17.899 mPa·s at 343 K. Like ILs, the application of DESs needs to address their viscosity issues.[90] Viscosity is related to the accumulation effects from intrinsic structures, van der Waals, electrostatic interactions, hydrogen bonds, molecular geometries and charge distribution.[91] Abbott *et al* previously explained the viscosity of a fluid using hole theory.[92] They ascribed this to the free volume and the probability of finding holes of suitable dimensions where ions can move in. The eutectics are composed of holes or vacancies, showing structural similarity to imidazolium based ILs.[93] It has been reported that ILs has relatively large radii about 3~4 Å compared to the average radius of the voids with a value of 2 Å that is chose to the radius of melt salts.[92] Normally, the probability of finding a hole for ILs is in the range of 10^{-4}-10^{-7} while approximately 1 for molten salts.[94] Compared with pure MEA, the probability of finding a hole for ILs is decrease when BMIMCl is added into MEA, which leads to an increase of the viscosity. For the DESs with different composition, our work presented at organic salt/HBD molar ratio dependence of the viscosity of the DESs. By tuning the BMIMCl/MEA molar ratio, a decrease of viscosity of DESs was observed with the increasing HBD molar concentration. For example at 298 K, viscosities of the eutectics were 132.68, 47.32 and 28.13 mPa·s for MEA:ILs(1:1), MEA:ILs(2:1) and MEA:ILs(4:1), respectively. Indeed, viscosity is related to the comprehensive accumulation of intrinsic structure, van der Waals, electrostatic, hydrogen bond, molecular geometry and charge distribution.[61, 91, 95] In general, it is significant that the viscosity of the above-mentioned DESs is obviously lower than those of common imidazole-based[96] or functionalized ILs labelled with lower viscosity[97, 98] and some binary eutectic solvents.[95, 99]

Thermal analysis of DESs

The decomposition temperature (T_d) of the DESs was investigated using a thermogravimetric analyzer (TGA). The results were summed in Table 1 and TGA curves are plotted in Fig. 7. It is clearly seen from Fig. 7 that BMIMCl has the good thermal stability while MEA exhibits the poor thermal stability. MEA shows a one-step weight loss: the onset of TGA curve occurs at 348 K with 5% weight loss and all weight loss occurs around 420 K. The weight loss of MEA is ascribed to its evaporation.

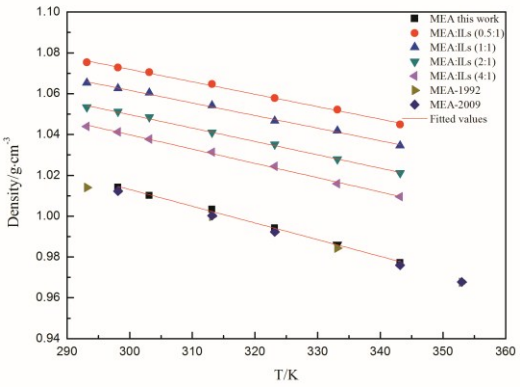

Fig. 5 Densities of MEA and DESs at different temperatures.

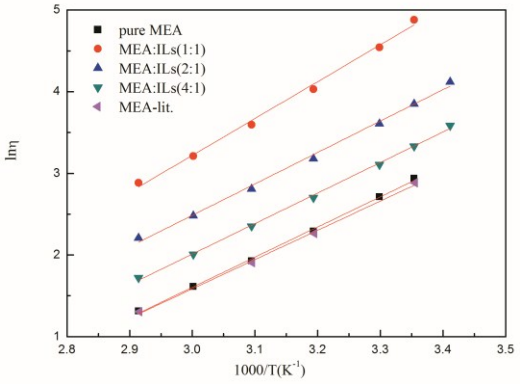

Fig. 6 Viscosities of MEA and DESs at different temperatures.

The onset of thermal decomposition of BMIMCl is recorded at 532 K with 18% weight loss and the decomposition completes around 582 K. All of the DESs curves show two-step weight loss. Take MEA:ILs(1:1) for example, the first onset of thermal decomposition occurs at 352 K, resulted mainly from MEA evaporation; and the second occurs at 533K, due to BMIMCl decomposition. The thermal stability of DESs ranks as: MEA:ILs(1:1) > MEA:ILs(2:1) > MEA:ILs(4:1) as the concentration of MEA increases, as Fig. 7 shows. This means a higher MEA concentration in DESs corresponds to a lower thermal stability of DESs.

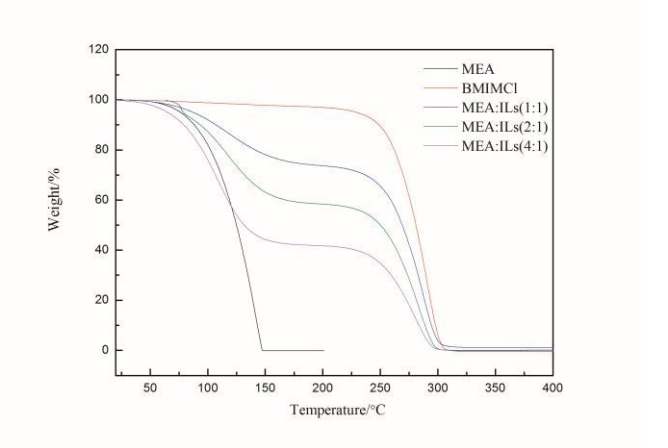

Fig. 7 TGA traces of MEA, BMIMCl and DESs.

Table 1 Thermal transition temperatures of the MEA, BMIMCl and DESs.

Sample	HBD/ILs Molar ratio	ILs wt %	T_g /K	T_m /K	[a]T_d /K
MEA	n/a	0	n/a	285.65	348
BMIMCl	n/a	100%	225	341.48	502
MEA:ILs(1:1)	1:1	74.1%	188.14	n/a	359
MEA:ILs(2:1)	2:1	58.8%	181.16	261.98	351
MEA:ILs(4:1)	4:1	41.7%	235.82	270.82	338

[a] T_d is defined as the temperature with the weight loss of 5%

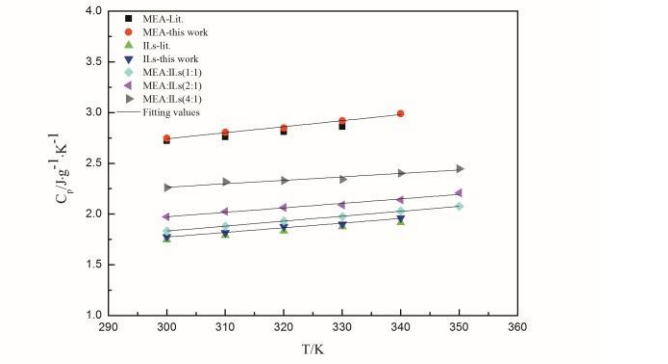

Fig. 8 Heat capacities of MEA, BMIMCl and DESs.

The melting points and glass transition temperatures of the DESs are presented in Table 1 (Further information can be found in Fig. S1-S5). The melting point is the onset of an endothermic peak on heating and glass transition temperature is taken as the midpoint of a small heat capacity change on heating from the amorphous glass to liquid state, respectively.[100] As Table 1 shows, the melting point of 341.48 K for BMIMCl is in good agreement with the literatures.[101] As mentioned above, the DESs are normally featured by a lower melting point than those of individual constituent. In this work, a depression of melting point of the DESs was achieved by adding MEA to BMIMCl. Except from MEA:ILs(1:1), the melting point of the eutectic mixture are 261.98 K for MEA:ILs(2:1) and 270.82 K for MEA:ILs(4:1). The melting point of the DESs is considerably lower than those of individual constituents. The significant depression of the freezing point stems from the hydrogen bond interaction between MEA molecule and the $BMIM^+$ cation.[28, 29, 61] When mixed with MEA, the hydrogen atoms on $BMIM^+$ ring are capable of forming hydrogen bonds with $-NH_2$ on the MEA, replacing the original C-H···Cl interaction and displaces Cl^- anion. The resultant hydrogen bonding formed through C_2 hydrogen causes redistribution of electron density on the ring, alters charge symmetry on $BMIM^+$, and perturbs the original Coulomb interaction between $BMIM^+$ and Cl^-. Fumino *etal* has made similar observation through studying imidazolium ILs.[102]

In a further study of thermal behavior, the heat capacities of pure MEA, BMIMCl and DESs are in Fig. 8. The experimental heat capacities of all samples increase with increasing temperature. In the whole temperature range, heat capacities follow a trend as BMIMCl < MEA:ILs(1:1) < MEA:ILs(2:1) < MEA:ILs(4:1) < MEA. It is evident from our findings that pure IL and the DESs exhibit lower heat capacity than MEA; and that adding MEA increases the heat capacity of DESs. It is worth noting that heat capacity of the DESs is less than 2.3 $J{\cdot}g^{-1}{\cdot}K^{-1}$, considerably lower than that of water (4.18 $J{\cdot}g^{-1}{\cdot}K^{-1}$). Superior to amine-based solvents, therefore, this kind of anhydrous solvents could successfully circumvent the high demand for sensible heat and inevitable evaporation of water in desorption process where the solvents are heated to release CO_2. Therefore, DESs provide a novel strategy to reduce the irrecoverable energy consumption and eventually offer energy-saving potentials for CO_2 capture.

Absorption uptake of CO_2

CO_2 absorption in DESs was evaluated at ambient pressure and temperature. CO_2 uptake in MEA was measured as for reference and satisfactory consistence was reached with literature.[103] CO_2 uptake in 30 wt% MEA aqueous solution is 13 wt%, corresponding to 0.61 mole CO_2 per mole MEA. The representative absorption curves *vs* bubbling time were presented in Fig. 9. The absorption in the first 5 hoursis highlighted in Fig. 10. CO_2 absorption in 30 wt% MEA aqueous solution reached equilibrium within 200 min, due to relatively fast gas diffusion and fast chemical reaction between primary amine group and CO_2. In contrast to MEA solution, CO_2 absorption in three eutectics was slower. The difference

between these situations is caused by the addition of ILs. First, the physical absorption through interactions between ILs and CO_2 is slow, which has been well acknowledged by many authors.[104-107] Furthermore, the absorption experiment is carried out under atmospheric pressure which has little facilitation to the physical absorption. Second, the viscosity has notable effect on the absorption kinetic: a higher viscosity corresponds to slower mass transfer. Therefore, CO_2 diffusion caused by the increased viscosity due to the addition of ILs,[54] which demands a longer time for the absorption to reach equilibrium.

As seen in Fig. 9, CO_2 absorption was fast in the first 20 mins, resulting in a sharp increase of CO_2 uptake. In the following time, CO_2 uptake proceeded slowly and steadily. The slope of these absorption curves can be used to evaluate the absorption rate. As seen in Fig. 9, the aqueous solution presents the steepest slope amongst the absorbents, which stands for a higher reaction rate than eutectics.

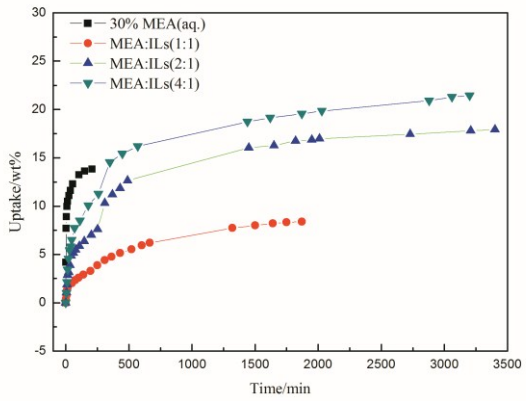

Fig. 9 CO_2 uptake as a function of bubbling time at room temperature.

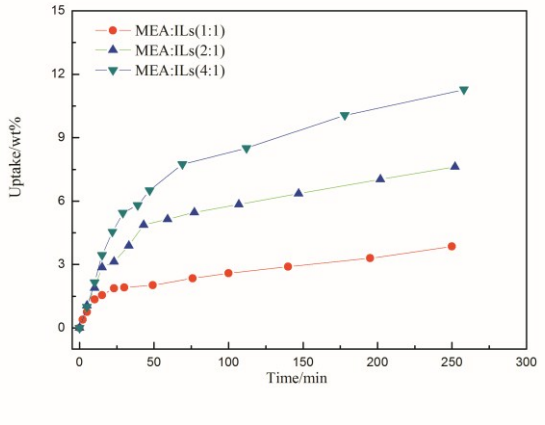

Fig. 10 CO_2 uptake in the initiate 5 hours at room temperature. CO_2 absorption in 30 wt % MEA is step-limiting due to the fast CO_2 diffusion. DESs are more viscous liquids and the the limitation of gas diffusion cannot be ignored. The gentle slope of the absorption curves for DESs reflects smaller gas diffusion during the whole absorption process. Also, physical absorption with BMIMCl may contribute to the overall CO_2 absorption, which will be analyzed by spectroscopic investigations in the following section.

The CO_2 uptake is compared with other DESs and ILs, shown in Table 2. CO_2 uptakes in pure MEA and 30% MEA aqueous solution are 30 wt% and 13 wt% in this study, respectively, in agreement with those of previous work.[26, 108] The IL/HBD molar ratio shows a remarkable influence on the final CO_2 uptake under equilibrium: the CO_2 uptakes in three DESs are 21.4% (MEA:ILs(4:1)), 17.9% (MEA:ILs(2:1)) and 8.4% (MEA:ILs(1:1)), respectively.

It can be seen from Table 2 that the gravimetric CO_2 capacity also exceeds those of conventional and functionalized ILs. For example, the CO_2 capacities have been reported to be 3.58% for [bmim][PF_6] and to be 18.5% in dual amino-functionalized cation-tethered ILs (DAIL), as exemplified in Table 2. ChCl based DESs as CO_2 solvents have been of interest in recent years. However, without incorporating nucleo-philic Lewis bases, ChCl containing DESs exhibit poor CO_2 capacity, e.g. less than 4% in a ChCl-Gly-DBU DES, albeit being measured at a high pressure up to 13 MPa, suggesting lack of chemical reaction with CO_2. The importance of incorporating nucleo-philic Lewis bases in the system is highlighted in an example of MEA-IL-Cl system that demonstrated a CO_2 absorption capacity up to 28.6%. In this system chloride anion can stabilize the protonated MEA, a coproduct of CO_2 absorption adduct, in organic solutions through hydrogen bonding, which facilitates CO_2 reaction to a greater degree.[54] In comparison our DESs provide the decent gravimetric CO_2 capacity up to 21.4%. Together with described above, these anhydrous system have low heat capacity. Therefore, the DESs highlight their potentials in CO_2 capture from the point of energy consumption.

Absorption mechanism of CO_2

In order to investigate the reactivity of the DESs, IR and NMR spectra were employed to analyze CO_2 absorption mechanism. The ATR-IR spectra of MEA:ILs(1:1) before and after reactingwith CO_2 are shown in Fig. 11. The IR spectra of other DESs before and after CO_2 absorption are shown in Fig. S6-S7. Fig. 11 clearly differentiates the chemically bonded and physically absorbed CO_2 in MEA:ILs(1:1). The new grown signal at 2958 cm^{-1} is the N-H stretch of carbamate cation and new signal at 1674 cm^{-1} can be ascribed to the asymmetric stretch of carbamate. Physically absorbed CO_2 is nominated at 2167 cm^{-1}, assigned to the asymmetric stretch of CO_2. Similar assignments of IR bands before and after CO_2 absorption can be found in MEA:ILs(2:1) and MEA:ILs(4:1).

The ^1H NMR spectra of fresh and CO_2 loaded MEA:ILs(1:1) were shown in Fig. 12 (The ^1H NMR spectra of other DESs before and after CO_2 absorption are shown in Fig. S8-S9). CD_3OD was used as the solvent for all samples.In comparison with the fresh DESs, some new peaks and shifts can be observed in the ^1H NMR spectra of CO_2 loaded DESs. The characteristic peak at 3.56 and 2.71 ppm of DESs shift

downfield to 3.70 and 2.96 ppm, respectively, after reacted with CO_2, implying the chemical reaction between DESs and CO_2. This finding is in good agreement with recent work.[83, 86] The downfield shifts can be elucidated by the concomitant accumulation of protonated MEA, in which the electron-withdrawing $–NH_3^+$ group can withdraw electron density. In addition, two new peaks appear at 3.55 and 3.15 ppm upon CO_2 loading. The two peaks correspond to the two CH_2 groups in the carbamate adduct. Importantly, the C_2H group shows a slight upfield shift from 9.15 to 9.06 ppm after CO_2 absorption. Adversary to downfield shift upon hydrogen bonding formation, the upfield shiftof C_2-H implies a breakdown of hydrogen bond that originally forms with MEA. These peaks of C_4H and C_5Halso shift upfield, i.e. from 7.72 ppm to 7.67 ppm for C_4H and from 7.65 ppm to 7.61 ppm for C_5H, respectively. This phenomenon may be caused by the deshielding effects as the increased acidity after CO_2 absorption.[83]

The ^{13}C NMR spectra of fresh and CO_2 loaded MEA:ILs(1:1) are shown in Fig. 13. The ^{13}C NMR spectra of MEA:ILs(2:1) and MEA:ILs(4:1) before and after CO_2 absorption are shown in Fig. S10-S11). Generally, the difference between ^{13}CNMR spectra of fresh and CO_2 loaded DESs adequately support the mechanism of conventional 2:1 amine to CO_2 stoichiometry. As discussed before, two characteristic peaks located in 43.48 and 63.29 ppm of DESs comes from MEA before CO_2 absorption. Three new peaks appeared at 41.89, 58.94 and 160.03 ppm implies the formation of carbamate after CO_2 bubbling,[83, 109] which confirms the chemically bonded CO_2. Meanwhile, the intensity of protonated MEA peak decreased and the peak upfield shifted from 63.29 to 62.12 ppm.Different from the significant upfield-shift observed in ^1H NMR spectra, the ^{13}C signals on $BMIM^+$, including C_2, C_4 and C_5, do not exhibit any shift. Interestingly, we observed the formation of carbonate/bicarbonate using D_2O as the solvent by NMR spectrum. It is possible that the formed carbamate could undergo hydrolysis in presence of D_2O. This observation implies that a higher CO_2 absorption capacity can be achieved by adding water, resulting in the formation of carbonate/bicarbonate. Herein, a mechanism is proposed as following for CO_2 absorption with MEA:ILs(2:1), seen in Scheme 1. In this mechanism, ILs behavior as medium that stabilize absorption product to improve CO_2 uptake through hydrogen bond. It should be noted that this mechanism is valid for MEA:ILs(1:1) and MEA:ILs(4:1). Wang *et al* also found that The TMG cation could interact with the CO_2 molecules to forming N–H···O hydrogen bonds.[10] A recent work has reported that the formation of hydrogen bond between chloride ion and protonated MEA facilitates CO_2 absorption.[54] These finds are supportive to our mechanism.

Table 2 CO_2 absorption capacities of different systems.

Systems	Temp./K	P /kPa	CO_2 uptake /wt%	Ref.
MEA:ILs(1:1)	298	100	8.4	this work
MEA:ILs(2:1)	298	100	17.9	this work
MEA:ILs(4:1)	298	100	21.4	this work
MEA(neat)	293	100	29.9	26
30wt% (aq.)	298	100	13	this work
30wt% (aq.)	313	101.3	12.8	108
ChCl : Glycerol (1:2)	303	187	0.64	45
ChCl : EG (1:2)	303	236	0.70	46
MEA : HIL: Cl^- (2:1:1)	308	100	28.6	54
ChCl : Gly : DBU(1:2:6)	298	100	3.55	110
ChCl:EG (1:4)	298	1000	1.33	42
ChCl:Urea (1:4)	298	1000	1.42	42
[bmim][PF_6]	313	1517	3.58	111
[N_{66614}][Met]	298	100	7.8	112
DAIL	303	100	18.5	25
[P_{66614}][Pro]	295	100	6.7	113

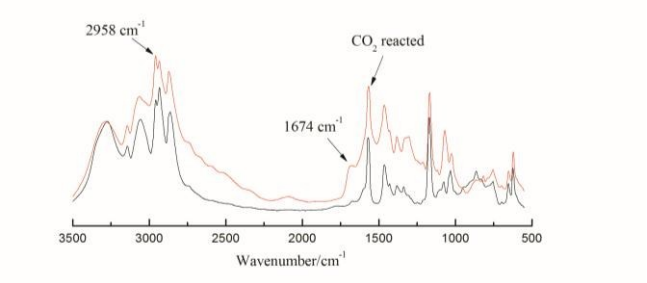

Fig. 11 CO_2 ATR-IR spectra of MEA:ILs(1:1) before and after CO_2 absorption.

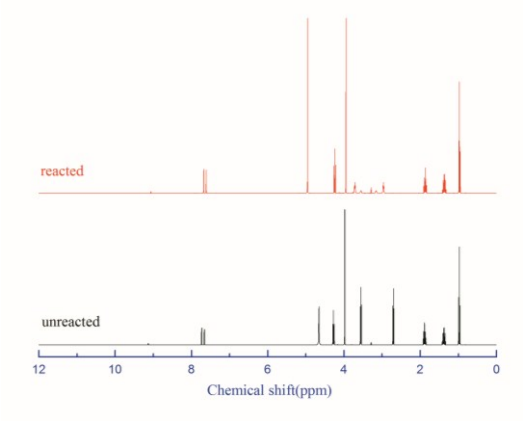

Fig. 12 ^{1}H NMR spectra of MEA:ILs(1:1) before and after CO_2 absorption.

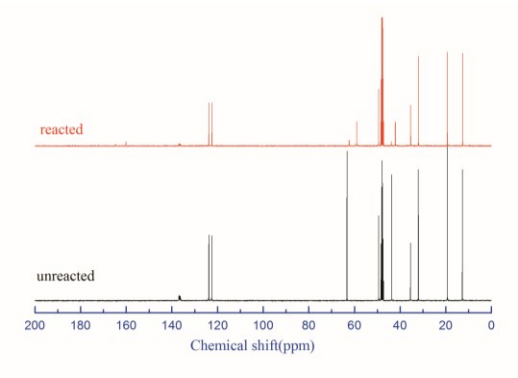

Fig. 13 ^{13}C NMR spectra of MEA:ILs(1:1) before and after CO_2 absorption.

Heat of CO_2 absorption in DESs

To confirm the accuracy of our method, the enthalpy of CO_2 in aqueous solution of MEA, MDEA and PZ are measured and compared our results with those of literatures,[60, 114] as shown in Fig. S13. The results showed that the experimental data are in good agreement with those in literatures except for MEA. As shown in Fig S13, the experimental enthalpy of CO_2 in MEA solution is slightly higher than that from Kim's group. Here, it should be pointed that, however, our results can well match that of Mayuri (the overall enthalpy of infinite dilution MEA solution and 30 wt % MEA at 313 K are -104.98 and -98.91 kJ·mol^{-1}).[115] The experimental enthalpies of CO_2 absorption in DESs and MEA solution are given in Fig. 14. As Fig. 14 shows, the enthalpies of CO_2 in these DESs depends on CO_2loading and decrease with the CO_2 loading, which shows the similar trendswith other solvents.[59, 60] Notably, the enthalpies of CO_2 in these DESs decrease gradually with the CO_2 loading from 0.05 to 0.4 mol CO_2/mol amine, which is especially in accordance with the amine or ILs-amine mixtures. As Fig. 14 shows, the enthalpy of CO_2 in MEA:ILs(4:1) and MEA:ILs(2:1) slightly decrease in the low CO_2 loading interval before 0.20~0.25. This means there is enough free MEA molecules to react with CO_2. With the CO_2 loading increases after 0.25 for MEA:ILs(2:1) and 0.30 for MEA:ILs(4:1), the enthalpies

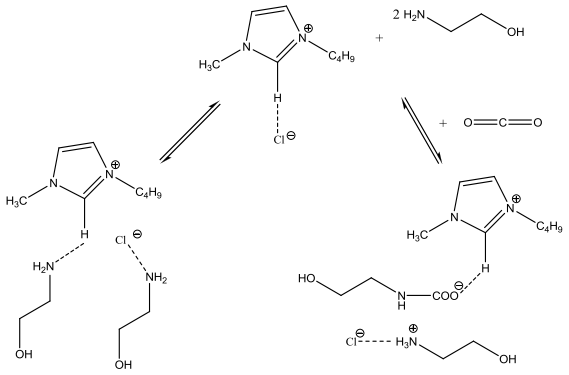

Scheme 1 The proposed mechanism between CO_2 and DESs.

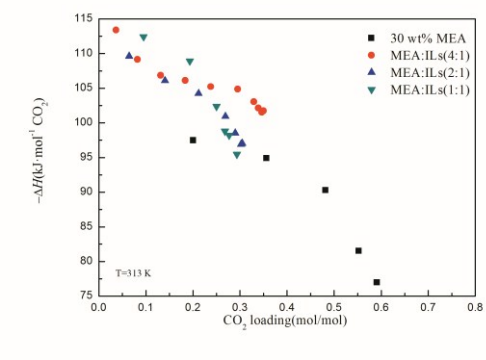

Fig. 14 Measured heat of CO_2 absorption with DESs at 313 K.

dramatically decrease, which implies the free MEA is depleting and the physical absorption of CO_2 in DESs dominates. Meanwhile, it is found that the experiment enthalpies of CO_2 in DESs are about 10% higher than that of 30 wt % MEA at 313 K. This can be explained by the following reasons. First, the of MEA in DESs are 58.31 wt % for MEA:ILs(4:1), 41.15 wt % for MEA:ILs(2:1) and 25.91 wt % for MEA:ILs(1:1), respectively. The higher concentration of MEA in DESs makes obvious contribution to the heat of absorption by chemical reaction between MEA and CO_2. Second, the hydrogen bond formed in DESs between the cation and the MEA molecule, shown in Scheme 1, influences the overall heat effects between CO_2 and DESs. Brennecke's group also draw the similar conclusion in MEA-ILs mixtures using COSMO-RS prediction.[116] This phenomenon is experimentally confirmed by Zhang's group using ILs tailored solvents.[59] Their results show that the intermolecular forces among CO_2, amine and ILs can change the thermodynamic behavior.[59] Our results show that the heat of CO_2 absorption in DESs can be tuned by choosing proper HBD and salt.

Conclusions

This work provides a comprehensive study of preparation, characterization of novel DESs and their efficiency in CO_2 uptake and heat of CO_2 absorption. Hydrogen bonds between MEA and ILs were observed in these thermally stable DESs, confirmed using IR, Raman and NMR spectroscopies. It is

found that the formation of hydrogen bond leads to a depression of melting point for DESs. In particular, CO_2 uptake reaches 21.4% for MEA:ILs(4:1) at room temperature and atmospheric pressure, which is higher than those of some ILs and choline chloride based DESs. The spectroscopic investigations demonstrate that CO_2 is physically absorbed and chemically bonded by the imidazolium-based DESs. Based on these observations, the proposed mechanism shows that ILs act as medium improving CO_2 uptake by hydrogen bond. Finally, the experimental heat of CO_2 absorption with DESs shows that reaction enthalpy can be tailored by changing the molar ratio of MEA and ILs. This anhydrous system offers insights on the promising cost-saving alternatives for CO_2 capture.

Acknowledgements

The authors sincerely appreciate the support by the Australian Academy of Technological Science and Engineering Joint Collaboration Group of Clean Coal Program, the National Natural Science Fund for Distinguished Young Scholars (No. 21425625), the Beijing Municipal Natural Science Foundation (NO. 2141003) and the International S&T Cooperation Program of China (2014DFA61670). The authors thank Dr. Anthony E. Rosamilia and Dr. Hanming Liu for their generous contributions in synthesis and discussion.

Notes and references

1. M. Y. He, Y. H. Sun and B. X. Han, *Angew. Chem. Int. Ed.*, 2013, **52**, 9620-9633.
2. G. T. Rochelle, *Science*, 2009, **325**, 1652-1654.
3. L. Cao, H. Dong, X. Zhang, S. Zhang, Z. Zhao, S. Zeng and J. Gao, *J. Chem. Technol. Biotechnol.*, 2015, **90**, 1918-1926.
4. U. E. Aronu, S. Gondal, E. T. Hessen, T. Haug-Warberg, A. Hartono, K. A. Hoff and H. F. Svendsen, *Chem. Eng. Sci.*, 2011, **66**, 6393-6406.
5. R. Idem, *Ind. Eng. Chem. Res.*, 2006, **45**, 2414 - 2420.
6. N. MacDowell, N. Florin, A. Buchard, J. Hallett, A. Galindo, G. Jackson, C. S. Adjiman, C. K. Williams, N. Shah and P. Fennell, *Energy Environ. Sci.*, 2010, **3**, 1645.
7. H. Lepaumier, *Ind. Eng. Chem. Res.*, 2009, **48**, 9061-9067.
8. X. Zhang, X. Zhang, H. Dong, Z. Zhao, S. Zhang and Y. Huang, *Energy Environ. Sci.*, 2012, **5**, 6668-6681.
9. M. Smiglak, J. Pringle, X. Lu, L. Han, S. Zhang, H. Gao, D. MacFarlane and R. Rogers, *Chem. Commun.*, 2014, **50**, 9228-9250.
10. Y. Wang, C. Wang, L. Zhang and H. Li, *Physical Chemistry Chemical Physics*, 2008, **10**, 5976-5982.
11. A. A. Oliferenko, P. V. Oliferenko, K. R. Seddon and J. S. Torrecilla, *Physical Chemistry Chemical Physics*, 2011, **13**, 17262-17272.
12. K. R. Seddon, *Pure Appl. Chem.*, 2000, **72**, 2275-2287.
13. D. R. MacFarlane, M. Forsyth, E. I. Izgorodina, A. P. Abbott, G. Annat and K. Fraser, *Phys. Chem. Chem. Phys.*, 2009, **11**, 4962-4967.
14. J. Zhu, F. Xin, J. Huang, X. Dong and H. Liu, *Chem. Eng. J.*, 2014, **246**, 79-87.
15. F. Endres and S. Z. El Abedin, *Physical Chemistry Chemical Physics*, 2006, **8**, 2101-2116.
16. M. Maase and K. Massonne, *Journal*, 2005, **902**, 126-132.
17. J. Huang and T. Rüther, *Aust. J. Chem.*, 2009, **62**, 298-308.
18. F. H. H. Olivier-Bourbigou, *Journal*, 2003, **92**, 67-84.
19. E. D. Bates, R. D. Mayton, I. Ntai and J. H. Davis, *J. Am. Chem. Soc.*, 2002, **124**, 926-927.
20. J. Zhang, S. Zhang, K. Dong, Y. Zhang, Y. Shen and X. Lv, *Chem. Eur. J.*, 2006, **12**, 4021-4026.
21. Y. Zhang, S. Zhang, X. Lu, Q. Zhou, W. Fan and X. Zhang, *Chem. Eur. J.*, 2009, **15**, 3003-3011.
22. B. E. Gurkan, J. C. de la Fuente, E. M. Mindrup, L. E. Ficke, B. F. Goodrich, E. A. Price, W. F. Schneider and J. F. Brennecke, *J. Am. Chem. Soc.*, 2010, **132**, 2116-2117.
23. C. Wang, X. Luo, H. Luo, D.-e. Jiang, H. Li and S. Dai, *Angew. Chem. Int. Ed.*, 2011, **50**, 4918-4922.
24. I. Niedermaier, M. Bahlmann, C. Papp, C. Kolbeck, W. Wei, S. K. Calderón, M. Grabau, P. S. Schulz, P. Wasserscheid and H.-P. Steinrück, *J. Am. Chem. Soc.*, 2014, **136**, 436–441.
25. J. Zhang, C. Jia, H. Dong, J. Wang, X. Zhang and S. Zhang, *Ind. Eng. Chem. Res.*, 2013, **52**, 5835-5841.
26. R. Vijayraghavan, S. J. Pas, E. I. Izgorodina and D. R. MacFarlane, *Phys. Chem. Chem. Phys.*, 2013, **15**, 19994-19999.
27. P. K. Koech, J. Zhang, I. V. Kutnyakov, L. Cosimbescu, S.-J. Lee, M. E. Bowden, T. D. Smurthwaite and D. J. Heldebrant, *RSC Adv.*, 2013, **3**, 566.
28. A. P. Abbott, G. Capper, D. L. Davies, R. K. Rasheed and V. Tambyrajah, *Chem. Commun.*, 2003, 70-71.
29. A. P. Abbott, D. Boothby, G. Capper, D. L. Davies and R. K. Rasheed, *J. Am. Chem. Soc.*, 2004, **126**, 9142-9147.
30. E. R. Cooper, C. D. Andrews, P. S. Wheatley, P. B. Webb, P. Wormald and R. E. Morris, *Nature*, 2004, **430**, 1012-1016.
31. A. P. Abbott, J. C. Barron, K. S. Ryder and D. Wilson, *Chem. Eur. J.*, 2007, **13**, 6495-6501.
32. R. B. Leron, A. Caparanga and M.-H. Li, *J. Taiwan. Inst. Chem. Eng.*, 2013, **44**, 879-885.
33. A. Yadav, S. Trivedi, R. Rai and S. Pandey, *Fluid Phase Equilib.*, 2014, **367**, 135-142.
34. Z. Maugeri and P. D. de María, *RSC Adv.*, 2012, **2**, 421-425.
35. A. P. Abbott, K. El Ttaib, G. Frisch, K. J. McKenzie and K. S. Ryder, *Physical Chemistry Chemical Physics*, 2009, **11**, 4269-4277.
36. T. P. S. Chao Wu, William F. Schneider, *Phys. Chem. Chem. Phys.*, 2012, **14**, 13163-13170.
37. D. Rengstl, V. Fischer and W. Kunz, *Physical Chemistry Chemical Physics*, 2014, **16**, 22815-22822.
38. D. V. Wagle, H. Zhao and G. A. Baker, *Acc. Chem. Res.*, 2014.
39. E. Durand, J. Lecomte and P. Villeneuve, *Eur. J. Lipid Sci. Technol.*, 2013, **115**, 379-385.
40. X. Li, M. Hou, B. Han, X. Wang and L. Zou, *J. Chem. Eng. Data*, 2008, **53**, 548-550.
41. X. Li, M. Hou, Z. Zhang, B. Han, G. Yang, X. Wang and L. Zou, *Green Chem.*, 2008, **10**, 879-884.
42. E. Ali, M. K. Hadj-Kali, S. Mulyono, I. Alnashef, A. Fakeeha, F. Mjalli and A. Hayyan, *Chem. Eng. Res. Des.*, 2014, **92**, 1898-1906.
43. Y. Chen, N. Ai, G. Li, H. Shan, Y. Cui and D. Deng, *J. Chem. Eng. Data*, 2014.

44. W. C. Su, D. S. H. Wong and M. H. Li, *J. Chem. Eng. Data*, 2009, **54**, 1951-1955.
45. R. B. Leron and M.-H. Li, *J. Chem. Thermodyn.*, 2013, **57**, 131-136.
46. R. B. Leron and M.-H. Li, *Thermochim. Acta*, 2013, **551**, 14-19.
47. Y.-P. Hsieh, R. B. Leron, A. N. Soriano, A. R. Caparanga and M.-H. Li, *J. Chem. Eng. Japan*, 2012, **45**, 939-947.
48. R. B. Leron and M.-H. Li, *Thermochim. Acta*, 2012, **530**, 52-57.
49. S. N. Aki, B. R. Mellein, E. M. Saurer and J. F. Brennecke, *J. Phys. Chem. B*, 2004, **108**, 20355-20365.
50. T. K. C. Jason E. Bara, Christopher J. Gabriel, Dean Camper, Alexia Finotello, Douglas L. Gin and Richard D. Noble, *Ind. Eng. Chem. Res.*, 2009, **48**, 2739–2751.
51. M. B. Shiflett, D. W. Drew, R. A. Cantini and A. Yokozeki, *Energy Fuels*, 2010, **24**, 5781-5789.
52. J. E. Bara, D. E. Camper, D. L. Gin and R. D. Noble, *Acc. Chem. Res.*, 2010, **43**, 152-159.
53. D. Camper, J. E. Bara, D. L. Gin and R. D. Noble, *Ind. Eng. Chem. Res.*, 2008, **47**, 8496-8498.
54. Q. Huang, Y. Li, X. Jin, D. Zhao and G. Z. Chen, *Energy Environ. Sci.*, 2011, **4**, 2125-2133.
55. S. Tsuzuki, H. Tokuda and M. Mikami, *Phys. Chem. Chem. Phys.*, 2007, **9**, 4780-4784.
56. R. P. Matthews, T. Welton and P. A. Hunt, *Physical Chemistry Chemical Physics*, 2014, **16**, 3238-3253.
57. K. Dong, S. Zhang, D. Wang and X. Yao, *J. Phys. Chem. A*, 2006, **110**, 9775-9782.
58. K. Dong, S. Zhang and Q. Wang, *Sci China Chem.*, 2010, **53**.
59. J. Gao, L. Cao, H. Dong, X. Zhang and S. Zhang, *Applied Energy*, 2015, **154**, 771-780.
60. J. Liu, S. Wang, H. F. Svendsen, M. U. Idrees, I. Kim and C. Chen, *Int. J. Greenhouse Gas Control*, 2012, **9**, 148-159.
61. Q. Zhang, K. De Oliveira Vigier, S. Royer and F. Jerome, *Chem. Soc. Rev.*, 2012, **41**, 7108-7146.
62. J. Wang, S. Zeng, L. Bai, H. Gao, X. Zhang and S. Zhang, *Ind. Eng. Chem. Res.*, 2014, **53**, 16832-16839.
63. R. Mesmer, C. Baes Jr and F. Sweeton, *Inorg. Chem.*, 1972, **11**, 537-543.
64. H. Liu, J. Huang and P. Pendleton, *Energy Procedia*, 2011, **4**, 59-66.
65. H. J. Emeléus and A. G. Sharpe, *Advances in inorganic chemistry and radiochemistry*, Academic Press, 1964.
66. Y. Jeon, J. Sung, D. Kim, C. Seo, H. Cheong, Y. Ouchi, R. Ozawa and H.-o. Hamaguchi, *J. Phys. Chem. B*, 2008, **112**, 923-928.
67. H.-C. Chang, J.-C. Jiang, C.-Y. Chang, J.-C. Su, C.-H. Hung, Y.-C. Liou and S. H. Lin, *J. Phys. Chem. B*, 2008, **112**, 4351-4356.
68. K. M. Dieter, C. J. Dymek, N. E. Heimer, J. W. Rovang and J. S. Wilkes, *J. Am. Chem. Soc.*, 1988, **110**, 2722-2726.
69. P. Suarez, S. Einloft, J. Dullius, R. De Souza and J. Dupont, *J. Chim. Phys.*, 1998, **95**, 1626-1639.
70. K. Buch, *Nature*, 1933, **131**, 688.
71. F. Xu, H. E. Goldbach, P. H. Brown, R. W. Bell, T. Fujiwara, C. D. Hunt, S. Goldberg and L. Shi, *Advances in plant and animal boron nutrition*, Springer, 2007.
72. A. Elaiwi, P. B. Hitchcock, K. R. Seddon, N. Srinivasan, Y.-M. Tan, T. Welton and J. A. Zora, *J. Chem. Soc., Dalton Trans.*, 1995, 3467-3472.
73. A. P. Abbott, R. C. Harris, K. S. Ryder, C. D'Agostino, L. F. Gladden and M. D. Mantle, *Green Chemistry*, 2011, **13**, 82-90.
74. V. Kempter and B. Kirchner, *J. Mol. Struct.*, 2010, **972**, 22-34.
75. J.-C. Lassègues, J. Grondin, D. Cavagnat and P. Johansson, *J. Phys. Chem. A*, 2009, **113**, 6419-6421.
76. S. Hayashi, R. Ozawa and H.-o. Hamaguchi, *Chem. Lett.*, 2003, **32**, 498-499.
77. M. Korolevich, V. Sivchik, N. Matveeva, R. Zhbankov, V. Lastochkina, M. Frenkel', A. Ladut'ko, A. Pavlov and E. Petryaev, *J. Appl. Spectrosc.*, 1987, **46**, 400-403.
78. E. R. Talaty, S. Raja, V. J. Storhaug, A. Dölle and W. R. Carper, *J. Phys. Chem. B*, 2004, **108**, 13177-13184.
79. R. Holomb, A. Martinelli, I. Albinsson, J.-C. Lassegues, P. Johansson and P. Jacobsson, *J. Raman Spectrosc.*, 2008, **39**, 793-805.
80. H. Katayanagi, S. Hayashi, H.-o. Hamaguchi and K. Nishikawa, *Chem. Phys. Lett.*, 2004, **392**, 460-464.
81. Y. Omura and T. Shimanouchi, *J. Mol. Spectrosc.*, 1975, **57**, 480-489.
82. M. Shukla, N. Srivastava and S. Saha, *J. Mol. Struct.*, 2010, **975**, 349-356.
83. G.-j. Fan, A. G. Wee, R. Idem and P. Tontiwachwuthikul, *Ind. Eng. Chem. Res.*, 2009, **48**, 2717-2720.
84. S. A. Dharaskar, M. N. Varma, D. Z. Shende, C. K. Yoo and K. L. Wasewar, *Sci. World J.*, 2013, **2013**.
85. A. A. Fannin Jr, L. A. King, J. A. Levisky and J. S. Wilkes, *J. Phys. Chem.*, 1984, **88**, 2609-2614.
86. A. García-Abuín, D. Gómez-Díaz, A. B. López, J. M. Navaza and A. Rumbo, *Ind. Eng. Chem. Res.*, 2013, **52**, 13432-13438.
87. K. Noack, P. S. Schulz, N. Paape, J. Kiefer, P. Wasserscheid and A. Leipertz, *Phys. Chem. Chem. Phys.*, 2010, **12**, 14153-14161.
88. R. L. Ralph M. DlGulllo, Steven T. Schaeffer, Laura L. Brasher, Amyn S. Tela *J. Chem. Eng. Date*, 1902, **37**, 239-242
89. E. L. Smith, A. P. Abbott and K. S. Ryder, *Chem. Rev.*, 2014.
90. Y. Zhao, Y. Huang, X. Zhang and S. Zhang, *Phys. Chem. Chem. Phys.*, 2015, **17**, 3761-3767.
91. P. Wasserscheid and W. Keim, *Angew. Chem. Int. Ed.*, 2000, **39**, 3772-3789.
92. A. P. Abbott, G. Capper and S. Gray, *ChemPhysChem*, 2006, **7**, 803-806.
93. Q. Zhang, K. D. O. Vigier, S. Royer and F. Jérôme, *Chem. Soc. Rev.*, 2012, **41**, 7108-7146.
94. A. P. Abbott, R. C. Harris and K. S. Ryder, *J. Phys. Chem. B*, 2007, **111**, 4910-4913.
95. Y. Liu, Y. Chen and Y. Xing, *Chin. Chem. Lett.*, 2014, **25**, 104-106.
96. J. G. Huddleston, A. E. Visser, W. M. Reichert, H. D. Willauer, G. A. Broker and R. D. Rogers, *Green chem.*, 2001, **3**, 156-164.
97. L. Zhang, Z. Zhang, Y. Sun, B. Jiang, X. Li, X. Ge and J. Wang, *Ind. Eng. Chem. Res.*, 2013, **52**, 16335-16340.
98. B. Gurkan, B. F. Goodrich, E. M. Mindrup, L. E. Ficke, M. Massel, S. Seo, T. P. Senftle, H. Wu, M. F. Glaser, J. K. Shah, E. J. Maginn, J. F. Brennecke and W. F. Schneider, *J. Phys. Chem. Lett.*, 2010, **1**, 3494-3499.
99. Y. Hou, Y. Gu, S. Zhang, F. Yang, H. Ding and Y. Shan, *J. Mol. Liq.*, 2008, **143**, 154-159.

100. J. M. Crosthwaite, M. J. Muldoon, J. K. Dixon, J. L. Anderson and J. F. Brennecke, *J. Chem. Thermodyn.*, 2005, **37**, 559-568.
101. O. Yamamuro, Y. Minamimoto, Y. Inamura, S. Hayashi and H.-o. Hamaguchi, *Chem. Phys. Lett.*, 2006, **423**, 371-375.
102. W. H. Organization, *Guidelines for drinking-water quality: First addendum to volume 1, Recommendations*, World Health Organization, 2006.
103. F. Y. Jou, A. E. Mather and F. D. Otto, *Can. J. Chem. Eng.*, 1995, **73**, 140-147.
104. C. Cadena, J. L. Anthony, J. K. Shah, T. I. Morrow, J. F. Brennecke and E. J. Maginn, *J. Am. Chem. Soc.*, 2004, **126**, 5300-5308.
105. F. Karadas, M. Atilhan and S. Aparicio, *Energy Fuels*, 2010, **24**, 5817 – 5828.
106. L. A. Blanchard, D. Hancu, E. J. Beckman and J. F. Brennecke, *Nature*, 1999, **399**, 28-29.
107. A. Yokozeki, M. B. Shiflett, C. P. Junk, L. M. Grieco and T. Foo, *J. Phys. Chem. B*, 2008, **112**, 16654-16663.
108. K. Shen and M. Li, *J. Chem. Eng. Data* 1992, **37**, 96-100.
109. A. Liu, R. Ma, C. Song, Z. Yang, A. Yu, Y. Cai, L. He, Y. Zhao, B. Yu and Q. Song, *Angew. Chem. Int. Ed.*, 2012, **51**, 11306-11310.
110. L. L. Sze, S. Pandey, S. Ravula, S. Pandey, H. Zhao, G. A. Baker and S. N. Baker, *ACS Sustainable Chem. Eng.*, 2014, **2**, 2117-2123.
111. L. A. Blanchard, Z. Y. Gu and J. F. Brennecke, *J. Phys. Chem. B*, 2001, **105**, 2437-2444.
112. S. Saravanamurugan, A. J. Kunov‐Kruse, R. Fehrmann and A. Riisager, *ChemSusChem*, 2014, **7**, 897-902.
113. J. F. Brennecke, *J. Am. Chem. Soc.*, 2010, **132**, 2116-2117.
114. X. Chen, F. Closmann and G. T. Rochelle, *10th International Conference on Greenhouse Gas Control Technologies*, 2011, **4**, 101-108.
115. C. Villagran, M. Deetlefs, W. R. Pitner and C. Hardacre, *Analytical Chemistry*, 2004, **76**, 2118-2123.
116. M. Gonzalez-Miquel, M. Massel, A. DeSilva, J. Palomar, F. Rodriguez and J. F. Brennecke, *J. Phys. Chem. B*, 2014, **118**, 11512-11522.